

Electrochemical formation and X-ray structure of the five-coordinated ruthenium(II) $[\text{RuCl}(\text{dppp})_2](\text{PF}_6)$ complex

Alzir Azevedo Batista*, Luiz Acacio Centeno Cordeiro**

Departamento de Química, Universidade Federal de São Carlos, CP. 676, 13560 São Carlos, SP (Brazil)

and Glaucius Oliva

Departamento de Física e Ciência dos Materiais, Instituto de Física e Química de São Carlos, CP. 369, 13560 São Carlos, SP (Brazil)

(Received April 14, 1992; revised August 21, 1992)

Abstract

The electrochemical oxidation of *trans*-chlorohydro-di-1,3-bis(diphenylphosphino)propaneruthenium(II), $[\text{HRuCl}(\text{dppp})_2]$, was studied at a platinum electrode in dichloromethane containing 0.1 mol/l tetrabutylammonium perchlorate (TBAP). The cyclic voltammogram shows two one-electron oxidation waves corresponding to the formation of Ru^{III} and Ru^{IV} species. To account for this observation and considering that the pH of the solution decreases during the experiment, an internal reduction of Ru^{IV} to Ru^{II} is proposed generating the five-coordinated $[\text{RuCl}(\text{dppp})_2]^+$ species. The X-ray structure of the $[\text{RuCl}(\text{dppp})_2](\text{PF}_6)$ complex, recrystallized from dichloromethane/diethyl ether was determined and found to have approximate C_{2v} symmetry about the metal center.

Introduction

Several complexes of the general formula *cis*- and *trans*- $[\text{MX}_2(\text{chelate})_2]$ (chelate = $\text{C}_2\text{H}_4(\text{PR}_2)_2$ (R = Me, Et or Ph), $\text{CH}_2(\text{PPh}_2)_2$ and *o*- $\text{C}_6\text{H}_4(\text{PEt}_2)_2$; X = halogen, SCN) and *trans*- $[\text{MHX}(\text{chelate})_2]$ (M = Ru, Os; X = Cl, Br, I, H, SCN, CN, NO_2 ; chelate = a chelating ditertiary phosphine), were prepared by Chatt and Hayter [1, 2]. Five-coordinated complexes of Ru^{II} were initially synthesized by Stephenson and Wilkinson [3]. The catalytic activity of $[\text{RuCl}_2(\text{PPh}_3)_3]$ and $[\text{HRuCl}(\text{PPh}_3)_3]$ in a variety of reactions [4] drew attention to this class of compounds and to the phosphine ligands.

The five-coordinated complexes of Ru^{II} , $[\text{RuCl}(\text{dppp})_2](\text{PF}_6)$ and $[\text{Ru}_2\text{Cl}_4(\text{dppb})_3]$, where dppp and dppb are 1,3-bis(diphenylphosphino)propane and 1,4-bis(diphenylphosphino)butane, respectively, were initially reported by Bressan and Rigo [5]. James *et al.* [6] obtained the coordinatively unsaturated five-coordinated complex $[\text{Ru}_2\text{X}_4\{(+)-(diop)\}_3]$ (X = Cl, Br; diop = 2,2 dimethyl-1,3-dioxolan-4,5-bis(methylene)-bis(diphenylphosphine)). The literature data show that d^6 complexes, when they can be induced to be five-coordinated, are best classified as square pyramidal [7]

which is in agreement with second-order Jahn–Teller arguments [8]. This was observed for the $[\text{RuCl}_2(\text{PPh}_3)_3]$ and $[\text{HRuCl}(\text{PPh}_3)_3]$ compounds having coordination numbers of five, which showed square pyramidal stereochemistries in the solid state [9, 10] and in solution [7], although distinguishing between square pyramidal (SP) and trigonal bipyramidal (TBP) stereochemistries is difficult because the two isomers possess C_{2v} symmetry [7]. For some five-coordinated $[\text{RuX}(\text{P-P})_2](\text{BPh}_4)$ complexes, where X = Cl or H and (P-P) is a diphosphine, taking into account their ^{31}P NMR spectra, trigonal-bipyramidal structures were proposed [11]. In this paper we present some electrochemical and structural properties of the five-coordinated $[\text{RuCl}(\text{dppp})_2]^+$ species.

Experimental

General procedures

The ruthenium complexes, $[\text{RuCl}(\text{dppp})_2](\text{PF}_6)$ or $[\text{RuCl}(\text{dppp})_2](\text{ClO}_4)$ and *trans*- $[\text{HRuCl}(\text{dppp})_2]$, were prepared and purified as described in the literature [5, 12]. All the chemicals employed were of reagent grade quality (Aldrich, Steam). Tetrabutylammonium perchlorate (Fluka purum), was recrystallized from ethanol/water and dried overnight, under vacuum, at 100 °C. Reagent grade solvents (Merck) were purified by dis-

*Author to whom correspondence should be addressed.

**Permanent address: Campus Universitário do Guamá, Laboratório de Química/Pesquisa, Cep. 66050, Belém-Pará, Brazil.

tilling repeatedly from phosphorus pentoxide, and stored over Linde 4 Å molecular sieves. Purified argon was used for the removal of dissolved oxygen.

Electrochemistry

All experiments were carried out at room temperature in freshly distilled dichloromethane containing 0.1 mol/l TBAP, using an EG & G PARC electrochemical system consisting of a model RE 0089 recorder, a model 173 potentiostat and a model 175 universal programmer. A three electrode system with resistance compensation (IR_u) was used throughout. The working and auxiliary electrodes were a stationary platinum foil and a wire, respectively. The reference electrode was Ag/AgCl, 0.1 mol/l TBAP in CH_2Cl_2 , a medium in which ferrocene is oxidized at 0.48 V; all potentials are referred to this electrode. In the voltammetric measurements the working electrode was a platinum foil, and a Luggin capillary probe was used. In the controlled potential electrolysis a platinum mesh was used as working electrode and the auxiliary electrode was separated from the solution by a sintered glass disk.

pH measurements

To measure the pH of the solution, a glass electrode was previously conditioned at the working solution conditions and a calibration curve was made. It is important to point out that in this circumstance the glass electrode responds satisfactorily. An Orion Research pH-meter model 601 A digital ionalyzer was used for these measurements.

UV-Vis spectra

The UV-Vis spectra were recorded with a Varian DMS-100 spectrophotometer.

Chromatographic analysis

The chromatographs were recorded with a CG-20 chromatographer coupled to a 2 m long, 3 mm copper column packed with 5 Å Linde molecular sieves. The column temperatures of the vaporizer and thermal detector were kept either at 50, 40 or 140 °C. The current intensity was fixed at 140 mA. Argon was used as the carrier gas at a flow rate of 0.3 ml s⁻¹.

X-ray structural determination

The recrystallization of the $[\text{RuCl}(\text{dppp})_2](\text{PF}_6)$ complex from dichloromethane/ether yielded red-violet crystals, whose structure was determined. The crystal data are summarized in Table 1 together with some experimental details. A single crystal of approximate dimensions 0.20 × 0.15 × 0.25 mm was used for data collection and cell determination on an Enraf-Nonius

TABLE 1. Crystal data, data collection details and structure refinement results for the $[\text{RuCl}(\text{dppp})_2](\text{PF}_6) \cdot \text{C}_4\text{H}_{10}\text{O}$ complex

Chemical formula	$[\text{RuCl}(\text{P}_2\text{C}_{27}\text{H}_{26})_2](\text{PF}_6) \cdot \text{C}_4\text{H}_{10}\text{O}$
Molecular weight	1180.52
Space group	$P2_1$
$F(000)$	1212
Lattice parameters	
a (Å)	11.652
b (Å)	15.011(1)
c (Å)	15.410(2)
β (°)	94.86(1)
V (Å ³)	2686(1)
Z	2
D_{calc} (g cm ⁻³)	1.46
Linear absorption coefficient, μ (cm ⁻¹)	5.42

CAD-4 diffractometer with graphite monochromatized Mo $K\alpha$ ($\lambda = 0.71073$ Å) radiation at room temperature. Unit-cell parameters were obtained from a least-squares refinement of the setting angles of 25 reflections in the θ range 0–23°. Intensity data were collected in the ω -2 θ scan mode up to $\theta_{\text{max}} = 23^\circ$, scan rate range 6.7–20° min⁻¹; 3773 reflections were measured of which 3622 were independent ($R_{\text{int}} = 0.021$; $-12 \leq h \leq 12$; $0 \leq k \leq 16$; $0 \leq l \leq 16$) and 2848 with $I > 3\sigma(I)$ were employed in the refinement procedure (497 parameters refined). Data were corrected for Lp and absorption effects (max. and min. transmission factors 1.066 and 0.927, using the method of Walker and Stuart [13]). The intensity of one standard reflection was essentially constant throughout the experiment.

The structure was solved using the Patterson methods and difference Fourier techniques. The crystal asymmetric unit is composed of one $[\text{RuCl}(\text{dppp})_2]^+$ species, one PF_6^- counter ion and one diethyl ether molecule. In the final cycles of least-squares refinement, all non-H atoms were treated anisotropically, the phenyl rings were refined as rigid groups and all hydrogen atoms were included as fixed contributors with a common isotropic temperature factor $B = 4.6$ Å². The function minimized was $\sum_w (|F_o| - |F_c|)^2$, where $w = (\sigma^2(F_o) + cF_o^2)^{-1}$, with $c = 0.001$, resulting in $R = 0.057$, $R_w = 0.059$ and $S = 1.51$. Maximum shift to e.s.d. ratio was 0.001 and the maximum and minimum electron densities in the final difference map were 1.21 and -0.52 Å⁻³, respectively. Final atomic coordinates for all non-H atoms are given in Table 2 and relevant bond distances and angles are given in Tables 3 and 4, respectively. Scattering factors for non-H atoms were taken from Cromer and Mann [14] with corrections for anomalous dispersion from Cromer and Liberman [15]; for H atoms from Stewart *et al.* [16]. Programs used: SHELX86 [17], SHELX76 [18] and ORTEP [19].

TABLE 2. Fractional atomic coordinates and isotropic temperature parameters (\AA^2) of $[\text{RuCl}(\text{dppp})_2](\text{PF}_6) \cdot \text{C}_4\text{H}_{10}\text{O}$

Atom	<i>x/a</i>	<i>y/b</i>	<i>z/c</i>	<i>B</i> _{iso}
Ru	0.3480(1)	0.1175(0)	0.2335(1)	2.50(3)
Cl	0.4817(4)	-0.0018(3)	0.2369(3)	4.9(1)
C(1)	0.165(1)	0.133(1)	0.0327(8)	3.5(5)
C(2)	0.056(1)	0.1392(9)	0.0823(9)	3.9(5)
C(3)	0.066(1)	0.192(1)	0.1644(9)	3.1(5)
P(1)	0.2888(3)	0.0764(3)	0.0838(2)	2.9(1)
C(111)	0.3992(7)	0.0904(7)	0.0055(5)	3.6(5)
C(112)	0.3656(7)	0.1038(7)	-0.0825(5)	5.4(6)
C(113)	0.4480(7)	0.1050(7)	-0.1431(5)	5.9(7)
C(114)	0.5641(7)	0.0928(7)	-0.1156(5)	6.8(8)
C(115)	0.5978(7)	0.0794(7)	-0.0275(5)	5.8(7)
C(116)	0.5153(7)	0.0782(7)	0.0330(5)	4.0(5)
C(121)	0.2556(8)	-0.0413(5)	0.0601(7)	3.3(5)
C(122)	0.3453(8)	-0.1030(5)	0.0711(7)	4.4(6)
C(123)	0.3223(8)	-0.1938(5)	0.0612(7)	5.5(7)
C(124)	0.2097(8)	-0.2230(5)	0.0403(7)	5.2(7)
C(125)	0.1201(8)	-0.1613(5)	0.0292(7)	7.5(9)
C(126)	0.1430(8)	-0.0705(5)	0.0392(7)	5.9(7)
P(2)	0.1604(3)	0.1430(2)	0.2539(2)	2.7(1)
C(211)	0.0892(7)	0.0349(5)	0.2656(7)	3.4(5)
C(212)	0.1456(7)	-0.0452(5)	0.2515(7)	4.7(6)
C(213)	0.0858(7)	-0.1256(5)	0.2531(7)	5.0(6)
C(214)	-0.0304(7)	-0.1260(5)	0.2688(7)	7.1(9)
C(215)	-0.0867(7)	-0.0459(5)	0.2829(7)	5.1(7)
C(216)	-0.0269(7)	-0.0345(5)	0.2813(7)	4.4(6)
C(221)	0.1110(7)	0.2035(6)	0.3483(5)	3.0(5)
C(222)	0.1094(7)	0.1598(6)	0.4280(5)	3.2(5)
C(223)	0.0785(7)	0.2060(6)	0.5010(5)	5.4(7)
C(224)	0.0493(7)	0.2960(6)	0.4943(5)	5.0(7)
C(225)	0.0509(7)	0.3398(6)	0.4146(5)	5.7(7)
C(226)	0.0817(7)	0.2935(6)	0.3415(5)	4.0(5)
C(1')	0.402(1)	0.247(1)	0.433(1)	3.4(5)
C(2')	0.431(1)	0.327(1)	0.380(1)	4.5(6)
C(3')	0.360(1)	0.342(1)	0.2942(9)	3.5(5)
P(3)	0.4208(3)	0.1362(3)	0.3829(2)	3.0(1)
C(311)	0.5740(6)	0.1110(8)	0.4133(6)	3.5(4)
C(312)	0.6571(6)	0.1782(8)	0.4193(6)	4.9(7)
C(313)	0.7718(6)	0.1574(8)	0.4446(6)	6.0(8)
C(314)	0.8034(6)	0.0695(8)	0.4640(6)	7.3(9)
C(315)	0.7203(6)	0.0024(8)	0.4580(6)	7.0(9)
C(316)	0.6056(6)	0.0232(8)	0.4327(6)	5.2(7)
C(321)	0.3564(8)	0.0593(7)	0.4583(6)	4.1(6)
C(322)	0.3415(8)	0.0837(7)	0.5438(6)	5.7(7)
C(323)	0.2898(8)	0.0246(7)	0.5986(6)	6.3(8)
C(324)	0.2530(8)	0.0588(7)	0.5677(6)	6.3(8)
C(325)	0.2679(8)	-0.0832(7)	0.4820(6)	6.1(8)
C(326)	0.3196(8)	-0.0241(7)	0.4273(6)	4.3(6)
P(4)	0.3867(3)	0.2626(2)	0.2089(2)	2.8(1)
C(411)	0.5400(6)	0.2796(6)	0.1986(7)	3.2(5)
C(412)	0.5773(6)	0.3663(6)	0.1847(7)	4.5(6)
C(413)	0.6945(6)	0.3838(6)	0.1814(7)	5.5(7)
C(414)	0.7743(6)	0.3146(6)	0.1920(7)	6.5(8)
C(415)	0.7370(6)	0.2279(6)	0.2059(7)	6.5(8)
C(416)	0.6198(6)	0.2104(6)	0.2092(7)	5.0(7)
C(421)	0.3245(8)	0.3193(6)	0.1115(5)	2.9(4)
C(422)	0.3730(8)	0.3048(6)	0.0330(5)	3.9(5)
C(423)	0.3248(8)	0.3448(6)	-0.0433(5)	4.9(6)
C(424)	0.2281(8)	0.3992(6)	-0.0411(5)	6.0(8)
C(425)	0.1795(8)	0.4137(6)	0.0374(5)	5.8(7)

(continued)

TABLE 2. (continued)

Atom	<i>x/a</i>	<i>y/b</i>	<i>z/c</i>	<i>B</i> _{iso}
C(426)	0.2278(8)	0.3737(6)	0.1137(5)	4.8(6)
P(5)	-0.0073(5)	0.0715(4)	0.7720(4)	6.3(2)
F(1)	0.109(2)	0.124(2)	0.790(1)	16.8(6)
F(2)	-0.116(1)	0.014(1)	0.747(1)	12.7(5)
F(3)	-0.070(3)	0.116(3)	0.841(2)	27.0(1)
F(4)	0.051(3)	0.027(2)	0.700(2)	23.0(1)
F(5)	0.041(2)	0.004(2)	0.839(2)	19.2(8)
F(6)	-0.047(2)	0.144(1)	0.703(1)	15.5(6)
C(4)	0.618(1)	0.087(1)	0.655(1)	5.0(4)
C(5)	0.634(3)	0.194(2)	0.674(2)	9.3(7)
O	0.518(2)	0.206(2)	0.667(2)	14.2(7)
C(6)	0.460(3)	0.293(2)	0.701(2)	12.5(9)
C(7)	0.350(2)	0.292(2)	0.691(2)	8.1(6)

TABLE 3. Interatomic bond distances (\AA) for the $[\text{RuCl}(\text{dppp})_2](\text{PF}_6) \cdot \text{C}_4\text{H}_{10}\text{O}$ complex

Ru-P(1)	2.431(4)
Ru-P(2)	2.267(4)
Ru-P(3)	2.402(4)
Ru-P(4)	2.263(3)
Ru-Cl	2.371(5)
C(1)-C(2)	1.54(2)
C(1)-P(1)	1.80(1)
C(2)-C(3)	1.49(2)
C(3)-P(2)	1.84(1)
C(1')-C(2')	1.51(2)
C(1')-P(3)	1.85(2)
C(2')-C(3')	1.52(2)
C(3')-P(4)	1.82(1)
P(1)-C(111)	1.849(9)
P(1)-C(121)	1.839(9)
P(2)-C(211)	1.838(8)
P(2)-C(221)	1.848(9)
P(3)-C(311)	1.846(8)
P(3)-C(321)	1.84(1)
P(4)-C(411)	1.825(8)
P(4)-C(421)	1.822(9)

Results and discussion

Cyclic voltammograms for the reduction of the $[\text{RuCl}(\text{dppp})_2](\text{PF}_6)$ complex are shown in Fig. 1. The reversible $\text{Ru}^{\text{II}} \rightarrow \text{Ru}^{\text{I}}$ reduction process observed at -0.90 V has been previously reported for the same complex [20] using a polarographic technique in diglyme where $E_{1/2}$ was found as -0.75 V versus SCE.

Figure 2 shows the cyclic voltammogram of the *trans*- $[\text{HRuCl}(\text{dppp})_2]$ complex. It is interesting to mention that the usual diagnostic criteria used in cyclic voltammetry [21] point out that the oxidation of Ru^{II} to Ru^{III} species occurs at 0.37 V and is reversible. In this case the cathodic wave is always present and the ratio of cathodic to anodic peak currents is very close to one. This first process can be better seen in Fig. 3. The

TABLE 4. Selected bond angles ($^{\circ}$) for the $[\text{RuCl}(\text{dppp})_2](\text{PF}_6) \cdot \text{C}_4\text{H}_{10}\text{O}$ complex

Ru-P(1)	87.8(1)	C(2)-C(1)-P(1)	118.0(1)
Cl-Ru-P(2)	139.8(1)	C(1)-C(2)-C(3)	116.0(1)
Cl-Ru-P(3)	83.6(1)	C(2)-C(3)-P(2)	115.0(1)
Cl-Ru-P(4)	126.2(1)	C(111)-P(1)-C(121)	97.2(4)
P(1)-Ru-P(2)	88.6(1)	C(2')-C(1')-P(3)	117.0(1)
P(1)-Ru-P(3)	171.2(1)	C(1')-C(2')-C(3')	117.0(1)
P(1)-Ru-P(4)	97.5(1)	C(2')-C(3')-P(4)	115.0(1)
P(2)-Ru-P(3)	96.5(1)	C(1')-P(3)-C(321)	103.3(6)
P(2)-Ru-P(4)	93.9(1)	C(311)-P(3)-C(321)	98.5(5)
P(3)-Ru-P(4)	89.4(1)	C(411)-P(4)-C(421)	100.8(4)
Ru-P(1)-C(1)	116.6(5)	C(211)-P(2)-C(221)	100.6(4)
Ru-P(1)-C(111)	115.7(3)		
Ru-P(1)-C(121)	118.1(3)		
Ru-P(2)-C(3)	119.0(5)		
Ru-P(2)-C(211)	108.2(3)		
Ru-P(2)-C(221)	124.1(3)		
Ru-P(3)-C(1')	117.3(5)		
Ru-P(3)-C(311)	118.3(3)		
Ru-P(3)-C(321)	113.7(3)		
Ru-P(4)-C(3')	117.4(5)		
Ru-P(4)-C(411)	111.1(3)		
Ru-P(4)-C(421)	121.1(3)		

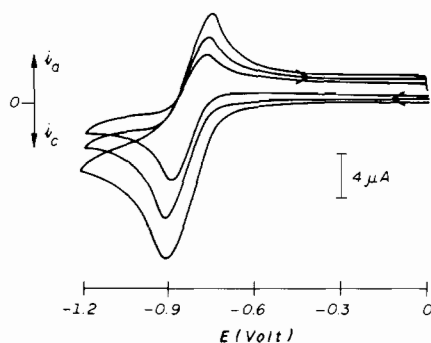


Fig. 1. Cyclic voltammogram for 10^{-3} mol/l $[\text{RuCl}(\text{dppp})_2](\text{PF}_6)$ in CH_2Cl_2 (0.1 mol/l in TBAP) measured at a platinum foil working electrode (1.19 cm^2). Scan rate: 100, 50 and 20 mV s^{-1} . Reference electrode: Ag/AgCl.

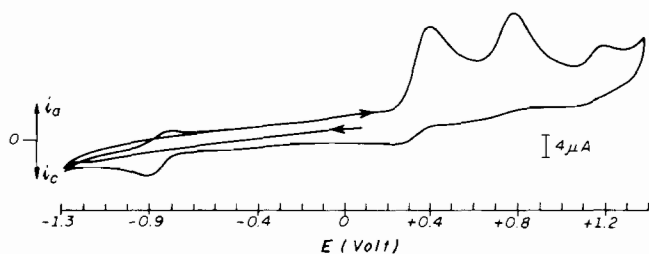


Fig. 2. Cyclic voltammogram of 10^{-3} mol/l *trans*- $[\text{HRuCl}(\text{dppp})_2]$ in CH_2Cl_2 (0.1 mol/l in TBAP) measured at a platinum foil electrode. Scan rate: 100 mV s^{-1} . Reference electrode: Ag/AgCl.

anodic peak at 1.20 V in the cyclic voltammogram of the *trans*- $[\text{HRuCl}(\text{dppp})_2]$ complex (Fig. 2) can be attributed to the coordinated diphosphine by comparison with the electrochemical behavior of the free diphosphine molecule (Fig. 4). This cyclic voltammogram is

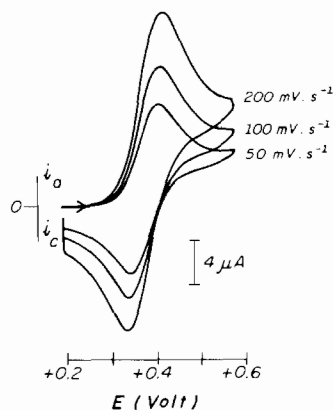


Fig. 3. Cyclic voltammogram of 10^{-3} mol/l *trans*- $[\text{HRuCl}(\text{dppp})_2]$ in CH_2Cl_2 (0.1 mol/l in TBAP) measured at a platinum foil electrode. Scan rate: 200, 100 and 50 mV s^{-1} . Reference electrode: Ag/AgCl.

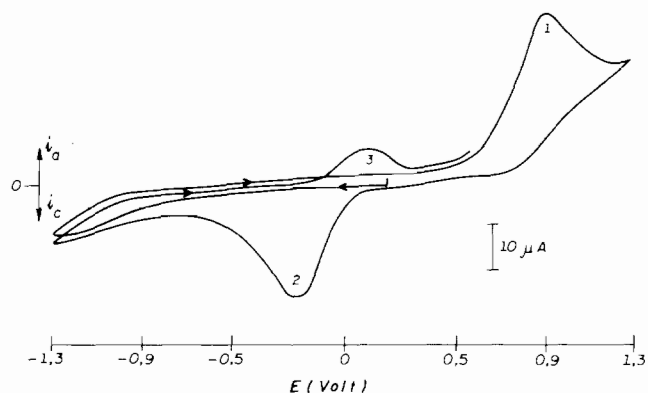
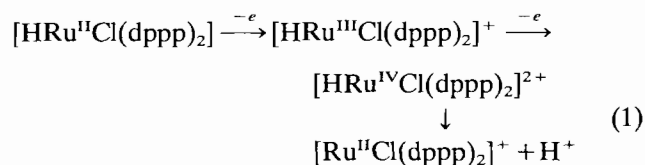


Fig. 4. Cyclic voltammogram of 1,3-bis(diphenylphosphino)propane in CH_2Cl_2 (0.1 mol/l in TBAP) measured at a platinum foil electrode. Scan rate: 100 mV s^{-1} . Reference electrode: Ag/AgCl.

very similar to that one obtained by Schiavon *et al.* [22] for free triphenylphosphine.

The anodic peak that appears near 0.80 V (Fig. 2) involves two processes: the first of them is electrochemical, followed by a chemical one. The electrochemical process is monoelectronic and may be attributed to the oxidation of Ru^{III} to Ru^{IV} . The chemical step in this process can be visualized as an internal reduction of the Ru^{IV} formed by the hydrido species coordinated to the metal. In this case all the processes involving the oxidation and reduction of the metal in this complex can be represented by eqn. (1)



As can be seen from this mechanism two monoelectronic steps are involved during the process and one proton is produced per *trans*- $[\text{HRuCl}(\text{dppp})_2]$ species.

Exhaustive controlled potential coulometry at 0.90 V yielded $n=2$ for this oxidation process and the pH of the solution decreased by approximately three units after the coulometric process (from pH 5.5 to 2.6) for a 10^{-3} mol/l solution of the complex. The formation of the five-coordinated $[\text{RuCl}(\text{dppp})_2]^+$ species in solution was followed by cyclic voltammetry as shown in Fig. 5. A comparison of Figs. 2 and 5 indicates that during the controlled potential coulometry process the peaks at 0.37 and 0.78 V decrease and the peak at -0.90 V (related to the five-coordinated complex) increases. After exhaustive controlled potential coulometry at 0.90 V the peaks related to the *trans*- $[\text{HRuCl}(\text{dppp})_2]$ complex disappear, suggesting that all of the six-coordinated complex was transformed to the five-coordinated species. These observations are also supported by the electronic spectra. Figure 6 shows the spectra of the five-coordinated complexes obtained by chemical and electrochemical methods.

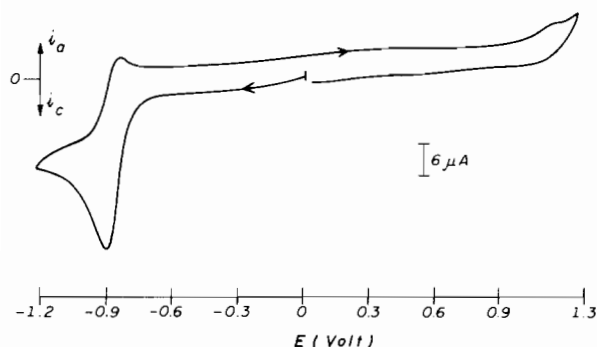


Fig. 5. Cyclic voltammogram of the five-coordinated $[\text{RuCl}(\text{dppp})_2]^+$ species obtained electrochemically from 10^{-3} mol/l *trans*- $[\text{HRuCl}(\text{dppp})_2]$ in CH_2Cl_2 (0.1 mol/l in TBAP) measured at a platinum foil electrode. Scan rate: 100 mV s^{-1} . Reference electrode: Ag/AgCl.

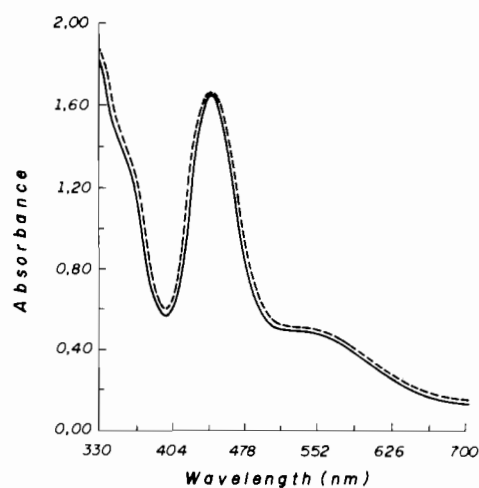
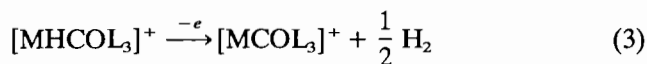
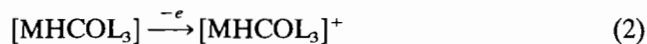


Fig. 6. Absorption spectra of the $[\text{RuCl}(\text{dppp})_2]^+$ (counter ion ClO_4^-) obtained by chemical (—) and electrochemical (---) ways in the near UV-Vis region measured in CH_2Cl_2 solution (10^{-3} mol/l).

of these two spectra, characterized by two peaks (550 and 447 nm) and a shoulder (360 nm) in the visible region due to d-d transitions, confirms the presence of the $[\text{RuCl}(\text{dppp})_2]^+$ species in both solutions.

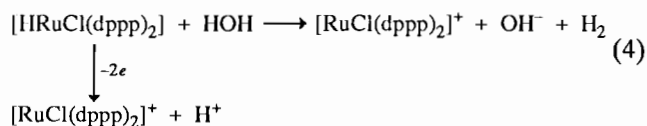
For the complexes $[\text{MHCOL}_3]$ ($\text{M} = \text{Rh}, \text{Ir}; \text{L} = \text{PPh}_3$) [23] similar one-electron oxidation processes were observed and the following reaction scheme was proposed



Another example of an electrochemically induced deprotonation has been recently reported [24] for *trans*- $[\text{HPtCl}(\text{PEt}_3)_2]$.

The $[\text{HRuCl}(\text{dppp})_2]$ complex was shown to be stable in dried dichloromethane solution for at least 6 h (a longer time than that spent during the electrolysis process), as detected by the presence of a typical symmetrical quintuplet at 17.95 ppm in the ^1H NMR spectrum of the complex in CDCl_3 [12].

It is interesting to mention that when non-dry solvent was used for the electrochemical measurements, apparently only one electron per *trans*- $[\text{HRuCl}(\text{dppp})_2]$ species was consumed during the controlled potential coulometry experiment. In order to understand this behavior the pH of the 10^{-3} mol/l solutions of the hydrido complex in the same conditions as the previous experiment was measured and found to be about 5.5 at the beginning of the experiment, increasing up to 7.8 after about 50 min. After this time, exhaustive controlled potential electrolysis of *trans*- $[\text{HRuCl}(\text{dppp})_2]$ at room temperature showed that the consumption of electrons corresponded to $n=1$, and the pH of the solution was equal to 6.2. These data are compatible with the fact that about 50% of the initial concentration of the *trans*- $[\text{HRuCl}(\text{dppp})_2]$ complex reacts with water resulting in the formation of molecular hydrogen according to eqn. (4)



Since the five-coordinated complex is electrochemically inert at 0.90 V (the applied potential for the coulometric measurements), two electrons were indeed consumed corresponding to 50% of the initial hydrido- Ru^{II} complex concentration, which was the electrochemical active species in solution.

It should be pointed out that, in principle, at the electrolysis potential, H_2 can be oxidized at the electrode but in the present case this was not experimentally observed. The evolved molecular hydrogen (according to eqn. (4)) was detected by gas chromatography.

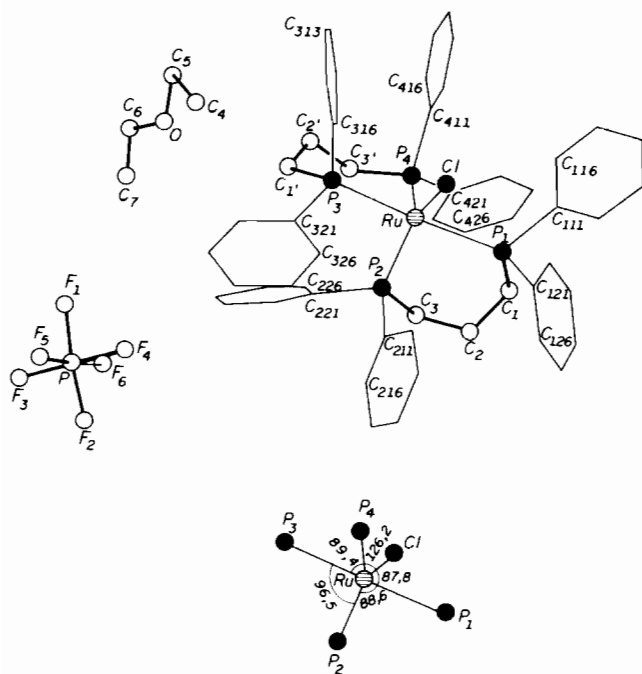


Fig. 7. Molecular structure and crystallographic numbering scheme for $[\text{RuCl}(\text{dppp})_2](\text{PF}_6) \cdot \text{C}_4\text{H}_{10}\text{O}$.

The ease of electrochemical formation of a five-coordinated compound from a six-coordinated complex containing diphosphine ligands in its structure seems to be very reasonable. Sullivan and Meyer [25] have reported that *trans*- $[\text{RuCl}_2(\text{dppm})_2]$ (dppm = bis-(diphenylphosphino)methane) isomerizes to the *cis*-isomer upon a one-electron oxidation.

The geometry of the five-coordinated complex determined by X-ray methods (Fig. 7) is trigonal bipyramidal with approximately local C_{2v} symmetry. The structure for this complex was proposed by McAuliffe and coworkers [11] from ^{31}P NMR data in CDCl_3 solution. These data contrast with the square pyramidal or C_{4v} structure proposed by Bressan and Rigo [5] for this five-coordinated Ru^{II} complex. They also contrast with Pearson's theoretical argument, based on second-order Jahn–Teller effects [8], which predicts the formation of a pyramidal structure from an octahedral hexacoordinated structure. Indeed in the hexacoordinated $[\text{RuCl}_2(\text{dppp})_2]$ complex, in solution, the two diphosphine ligands are very rigid [11] and with the formation of the five-coordinated $[\text{RuCl}(\text{dppp})_2]^+$ species the conformation is changed to a more stable C_{2v} structure.

The fact that the $[\text{RuCl}_2(\text{PPh}_3)_3]$ complex has square-pyramidal stereochemistry in the solid state and in solution, while $[\text{RuCl}(\text{dppp})_2](\text{PF}_6)$ is trigonal-pyramidal in both states confirms the fundamental importance

of the ligand in determining the stereochemistry of five-coordinated d^6 species [7] which can be very important for the reactivity of these complexes. Probably due to steric effects of the diphosphine ligands around the ruthenium ion the $[\text{RuCl}(\text{dppp})_2](\text{PF}_6)$ complex is inert to reactions with molecules such as pyridine, imidazole and triethylphosphite under mild conditions.

Supplementary material

Fractional atomic coordinates and isotropic temperature parameters, anisotropic thermal parameters and the complete interatomic bond distances and angles are available from the authors on request.

Acknowledgements

The authors thank CAPES and CNPq for financial support. They are also indebted to Dr Romeu C. Rocha-Filho for reading the English manuscript.

References

- 1 J. Chatt and R. G. Hayter, *J. Chem. Soc.*, (1961) 896.
- 2 J. Chatt and R. G. Hayter, *J. Chem. Soc.*, (1961) 2605.
- 3 T. A. Stephenson and G. Wilkinson, *J. Inorg. Nucl. Chem.*, 28 (1966) 945.
- 4 P. W. Armit and T. A. Stephenson, *J. Organomet. Chem.*, 57 (1973) C80.
- 5 M. Bressan and P. Rigo, *Inorg. Chem.*, 14 (1975) 2286.
- 6 B. R. James, D. K. W. Wang and R. F. Voigt, *Chem. Commun.*, (1975) 574.
- 7 P. R. Hoffman and K. G. Caulton, *J. Am. Chem. Soc.*, 97 (1975) 4221.
- 8 R. G. Pearson, *J. Am. Chem. Soc.*, 91 (1969) 4947.
- 9 A. C. Skapski and P. G. H. Troughton, *Chem. Commun.*, (1968) 1230.
- 10 S. J. La Placa and J. A. Ibers, *Inorg. Chem.*, 4 (1965) 778.
- 11 J. C. Briggs, C. A. McAuliffe and G. Dyer, *J. Chem. Soc., Dalton Trans.*, (1984) 423.
- 12 B. R. James and D. K. W. Wang, *Inorg. Chim. Acta*, 19 (1976) L17-L18.
- 13 N. Walker and D. Stuart, *Acta Crystallogr., Sect. A*, 39 (1983) 158.
- 14 D. T. Cromer and J. B. Mann, *Acta Crystallogr., Sect. A*, 24 (1968) 321.
- 15 D. T. Cromer and D. Liberman, *J. Chem. Phys.*, 53 (1970) 1891.
- 16 R. F. Stewart, E. R. Davidson and W. T. Simpson, *J. Chem. Phys.*, 42 (1965) 3175.
- 17 G. M. Sheldrick, *SHELX-86*, program for crystal solution. University of Göttingen, Germany, 1986.
- 18 G. M. Sheldrick, *SHELX-76*, program for crystal structure determination, University of Cambridge, UK, 1976.

- 19 C. K. Johnson, *ORTEP, Rep. ORNL-3794*, Oak Ridge National Laboratory, TN, USA, 1965.
- 20 G. Zotti, G. Pilloni, M. Bressan and M. Martelli, *J. Electroanal. Chem.*, **75** (1977) 607.
- 21 A. J. Bard and L. R. Faulkner, *Electrochemical Methods Fundamentals and Applications*, Wiley, New York, 1980, pp. 720.
- 22 G. Schiavon, S. Zecchin, G. Cogoni and G. Bontempelli, *J. Electroanal. Chem.*, **48** (1973) 425.
- 23 S. Valcher, G. Pilloni and M. Martelli, *J. Electroanal. Chem.*, **42** (1973) App. 5.
- 24 L. Chen and J. A. Davies, *Inorg. Chim. Acta.*, **175** (1990) 41.
- 25 B. P. Sullivan and T. J. Meyer, *Inorg. Chem.*, **21** (1982) 1037.